

CHROM. 4875

## A STUDY OF THE FLAME IONISATION DETECTOR

I. G. McWILLIAM\*

*Chemistry Department, Monash University, Clayton, Victoria 3168 (Australia)*

(Received June 11th, 1970)

## SUMMARY

At high concentration levels the linearity of response of the flame ionisation detector is dependent on the hydrogen flow rate, and at high hydrogen-nitrogen ratios marked non-linearity may be observed. Anomalous effects may also occur as a result of contamination of the flame jet. For *n*-heptane an essentially linear response has been obtained up to approximately 60  $\mu\text{g}/\text{sec}$  under optimum flow conditions. Under the same conditions toluene exhibits non-linearity at approximately 10  $\mu\text{g}/\text{sec}$ , but the linear range for toluene can be extended by increasing the hydrogen-nitrogen ratio. The construction and performance of the detector, amplifier and gas blending system used for the above investigations are discussed. A general expression is given relating current and applied voltage for the flame ionisation detector.

## INTRODUCTION

The two most important properties of the flame ionisation detector (FID) are its high sensitivity and its linearity of response. The latter has been established over a wide additive mass flow range, almost  $10^8$  to 1, by the use of various gas dilution systems<sup>1-4</sup>. However, doubts still remain as to whether exact linearity is achieved, particularly at the higher concentration levels. The present work is concerned mainly with linearity at high concentrations, and was undertaken as a preliminary investigation necessary for the study of peak shapes in gas chromatography.

Deviation from linearity over a wide concentration range should be evident from the slope of a log-log plot of signal output *versus* additive flow rate. The slope of this curve, which has been termed the "response index"<sup>3,4</sup>, should be 1.00 if exact linearity is achieved. Typical values reported in practice for the FID are 0.98-1.02 but the results suggest that this deviation is due to experimental error rather than to a basic non-linearity of the detector itself<sup>3,5,6</sup>. The main problem lies in the reliability of methods for generating low concentrations of organic vapours, since there is at present no reference device with which these can be checked. A diffusion dilution system which should give a logarithmic decrease in vapour concentration with time would appear

\* Present address: Department of Applied Chemistry, Swinburne College of Technology, John Street, Hawthorn, Victoria 3122, Australia.

to be an ideal reference system, but adsorption problems limit the usefulness of this approach<sup>7,8</sup>. The work reported below employed a direct gas blending system.

## EXPERIMENTAL

### Apparatus

The apparatus consisted of an insulated jet FID, a variable voltage supply to provide the jet potential, an electrometer amplifier and recorder, and a gas blending system for the introduction of controlled amounts of organic materials into the flame. The study is concerned mainly with a detector burning a mixture of both hydrogen and nitrogen at the jet but some results using hydrogen only are included.

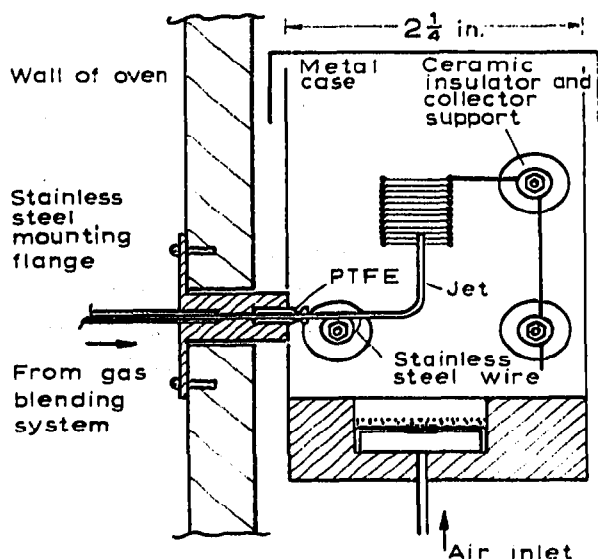


Fig. 1. Flame assembly (cross-sectional view).

The flame assembly is shown in Fig. 1. The main features are the use of a filled PTFE (polytetrafluoroethylene, Teflon) connector to insulate the 20 g stainless-steel jet from earth, the complete separation of the air inlet and jet assembly, and the construction of the collector electrode from heavy gauge wire. The jet, which forms one electrode, is at the axial centre of the cylindrical collector electrode, and the detector can be considered to have cylindrical symmetry. Collector electrodes of different diameters, required for a study of current *versus* voltage relationships, were made by winding 16 g tin-coated copper wire onto suitably sized formers, *e.g.* the shank of a drill. For most of the work reported here an internal diameter of 13 mm was used, an overall length of 15 mm, and the jet projected 2 mm above the bottom of the collector electrode.

The air distributor consisted of two layers of 120 mesh stainless-steel gauze supported on one layer of 18 mesh gauze. A spider support, or baffle, prevented direct flow of air from the centre of the distributor. To avoid disturbing the electrical field within the electrode assembly no internal ignition system was used. The flame was lit with a Toshiba type G-6 battery-operated gas lighter after removing the lid of the flame chamber. Due to the large cross-sectional area of the chamber (2 1/4 in.

square) a relatively large air flow rate was required to reach the signal maximum. However, the effect of air flow rate was quite flat and there was no evidence of turbulence, the signal stability at a fixed level of addition of organic material being excellent. Using both *n*-heptane and carbon tetrachloride at high concentrations as reference materials, the signal maximum was reached at an air flow rate of 1.0 l/min and remained constant up to at least 2.5 l/min. The detector was normally operated at a flow rate of 1.6 l/min. In comparison, a typical figure at which the maximum is reached with more compact detectors is 0.5 l/min<sup>1,3,6</sup>. At 0.3 l/min the signal obtained with the detector described here was 89% of the maximum for both *n*-heptane and carbon tetrachloride, and 76% for *n*-heptane at almost zero air flow rate.

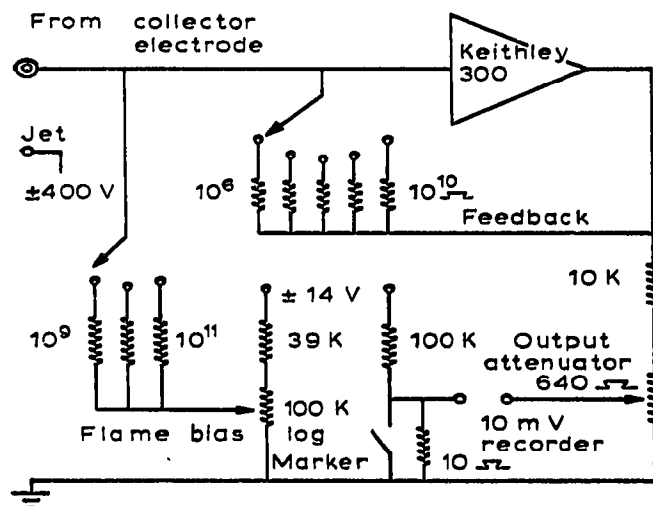


Fig. 2. FID amplifier circuit.

The circuit of the amplifier is shown in Fig. 2. This is based on a Keithley Model 300 operational amplifier (Keithley Instruments Inc., Cleveland, Ohio) which uses electrometer input tubes. The output attenuator resistor chain (640  $\Omega$  total) was divided into steps of 1, 2, 4, .. 64, and the feedback resistors provided four further factors of 10, a total range of  $6.4 \times 10^5$  to 1 for full scale deflection. Overall gain of the circuit was 0.64. With a Varian G-1000 10 mV recorder the noise level was about 0.5% of full scale at the maximum sensitivity setting (equivalent to  $1.6 \times 10^{-11}$  A full scale) and drift at this sensitivity was less than 1% per hour. At relatively low gas flow rates (30 ml/min nitrogen, 15 ml/min hydrogen) the background current due to the flame amounted to  $1.4 \times 10^{-11}$  A, this being caused mainly by impurities in the gas supplies<sup>9</sup>. Noise and short term drift (over a period of about 10 min) at an applied voltage of 380 V (positive jet) was less than  $3 \times 10^{-13}$  A. These figures were obtained using combustion air taken directly from the laboratory compressed air supply, with a coarse charcoal filter to remove dust and oil droplets. Provision was made for the jet voltage to be varied over the range  $\pm 380$  V in steps of approximately 27 V, or over the range  $\pm 38$  V in steps of approximately 2.7 V with an additional voltage divider. This is not shown in Fig. 2. In series with the voltage supply was a 1 M $\Omega$  protective resistor which prevents the voltage supply being overloaded in the event of an external short-circuit, and also protects unwary personnel who may ac-

cidentally touch the high voltage connections. Also not shown in Fig. 2 is an external zero control which is described in the operating instructions supplied with the Keithley operational amplifier.

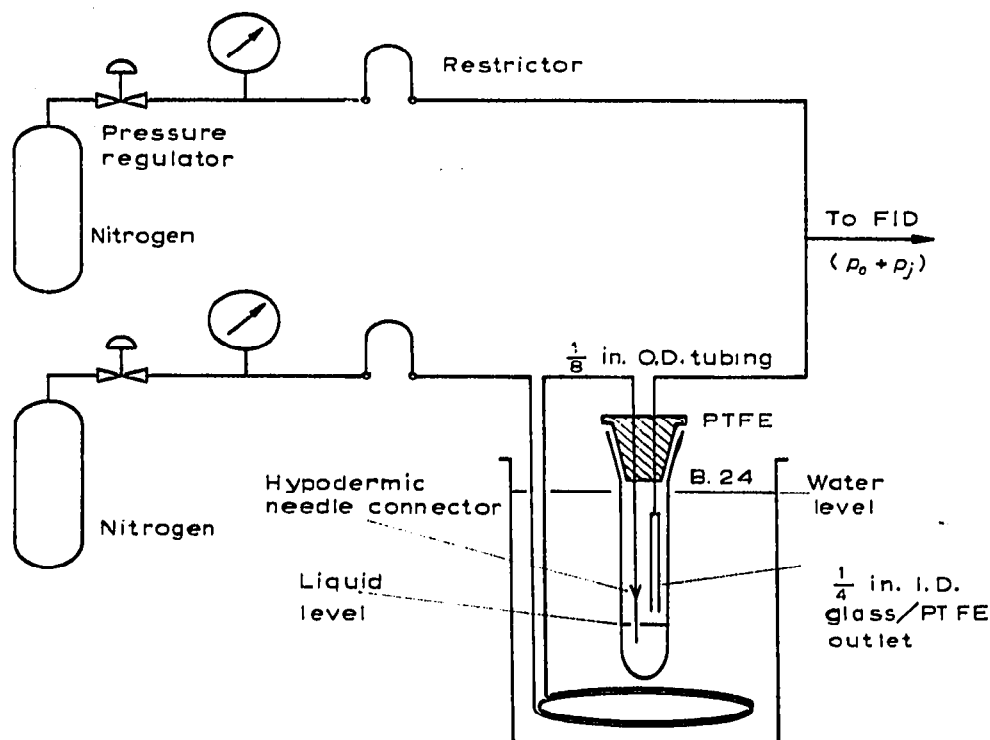


Fig. 3. Gas blending system.

The gas blending system is shown in Fig. 3. It consisted of two separate gas flow control systems and a saturator. The top of the saturator insert was made from PTFE with thin sealing rings to fit the B24 ground glass joint. However, even with careful machining, a thin layer of grease was found necessary to ensure a leak tight seal. By changing the grease when the liquid in the saturator was changed, cross-contamination problems were avoided. The interchangeable restrictors consisted of fixed lengths of  $1/8$  in. O.D.,  $1/16$  in. I.D., tubing filled with 60–80 mesh glass beads (F & M Scientific Corp., Avondale, Pa.). Typical flow rate figures for nitrogen, for a 5 in. length of 60–80 mesh beads and inlet pressures of 5 and 30 p.s.i.g. are 6 and 60 ml/min, respectively. By calibrating with a soap film flow meter the flow through the saturator could be varied while the total flow was kept constant. A similar flow arrangement has been used in the past for calibrating analysers<sup>10</sup> and in earlier investigations of the FID<sup>2</sup>. More recently the accuracy of the method has been discussed in some detail<sup>11</sup>. The hydrogen flow to the detector is controlled in a similar way, the restrictor this time being a 5 in. length of  $1/16$  in. I.D. tubing filled with 230–320 mesh glass beads. Flow rate figures in this case are approximately 15 and 155 ml/min for 5 and 30 p.s.i.g. In over eight years use these restrictors have been found to be far more reliable and reproducible than capillaries, being free from blocking problems to which fine capillaries are particularly susceptible. The air flow restrictor consisted of a 5 in. length of 20 g hypodermic needle

tubing with an inlet pressure of 6–10 p.s.i.g. In all cases Watts type 215 low flow low pressure precision regulators (Watts Regulator Co., Lawrence, Mass.) were used for pressure control, the large diaphragm area of these regulators providing precise control and freedom from oscillation.

The main problems encountered with the gas blending system are the saturator efficiency and the backpressure due to the restriction imposed on the gas flow by the detector jet. These are discussed in the next section.

#### *Performance of the gas blending system*

The efficiency of the saturator sets the eventual limit for the usefulness of a system of the type described above. TURNER AND CRUM<sup>12</sup> have used a simple saturator for high boiling liquids, and compounds which are solid at ambient temperature, in which the carrier gas passes over the surface of the liquid. They found that in the case of their saturator, and maleic anhydride as the sample, the flow rate of carrier gas was limited to about 12 ml/min for complete equilibration to be achieved.

In attempting to use the same system for samples which are volatile at room temperature, unsatisfactory results were obtained at flow rates much lower than this if the carrier gas merely passed over the surface of the liquid. For this reason the inlet line was terminated with a "Record" taper to which a 25 g hypodermic needle was fitted. The fine needle, positioned below the liquid surface, provided both good contact between the carrier gas and the liquid, and stirring to minimise temperature gradients. At low flow rates the small bubble size also minimises the flow rate variations resulting from bubble formation.

Results obtained with *n*-heptane, *n*-hexane and diethyl ether are shown in Fig. 4, the gas concentration in the effluent gas stream being determined by passing the saturated gas through a gas sampling valve (Carle Instrument Co., Fullerton, Calif.) fitted to a gas chromatograph. As shown by the results for *n*-hexane, the departure from equilibrium is very marked in the absence of the outer water jacket. However, the tendency towards a finite lower limit at high carrier flow rates, and a slow rate of recovery when the flow rate was reduced, suggested that the effect was predomi-

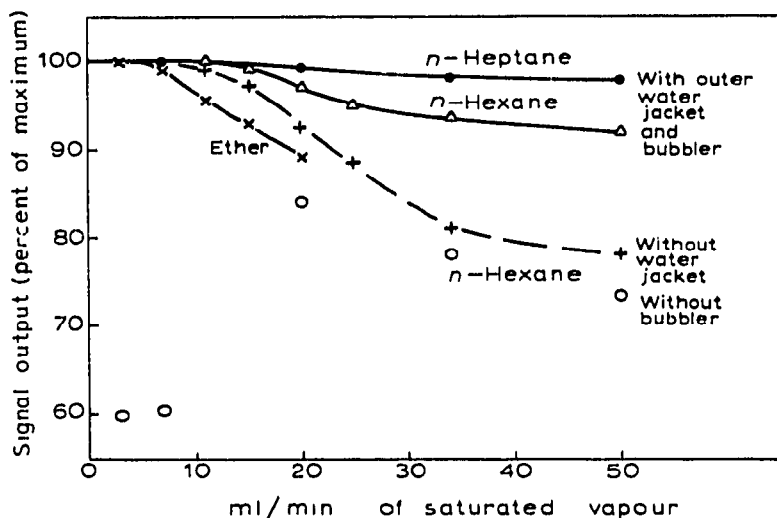


Fig. 4. Variation of saturator efficiency with gas flow rate.

nantly due to evaporative cooling of the liquid sample. Improved temperature stability was obtained with the outer water jacket, and the difference at high and low flow rates could be accounted for by the measured fall in temperature of the sample. Since only low flow rates (less than 11 ml/min) were involved in the present investigation the performance of the saturator was adequate, but it would appear that satisfactory results at higher flow rates and with more volatile samples such as ether (see Fig. 4) could be obtained by further improving heat transfer to the sample.

In the absence of the needle bubbler the results depend on the geometry of the system. In the particular case shown in Fig. 3, removal of the needle results in very inefficient vapour pickup at low flow rates, but there is a marked improvement as the stream of carrier gas impinges more forcibly on the liquid surface. This effect is shown for *n*-hexane by the separate points in Fig. 4.

The error due to the backpressure at the jet can be estimated as follows. The flow through a bed of granular material is related to the inlet pressure  $p_i$  and outlet pressure  $p_o$  by the expression

$$F_o = \frac{B_o A}{2\eta L} \left( \frac{p_i^2 - p_o^2}{p_o} \right) \quad (1)$$

where  $F_o$  is the flow rate measured at the outlet pressure,  $B_o$  is the specific permeability coefficient which is characteristic of the bed,  $\eta$  is the gas viscosity,  $A$  is the cross-sectional area of the bed, and  $L$  is its length<sup>13</sup>. Consider now the situation shown in Fig. 3 where there is a constant total flow to the detector, and the backpressure due to the jet is  $p_j$ . The mass flow of additive to the detector is determined by the volume flow rate ( $F_j$ ) of carrier gas passing through the saturator, the molecular weight of the additive ( $M$ ), and its partial vapour pressure,  $p/(p_o + p_j)$ , *i.e.*, by the function

$$F_j M \left( \frac{p}{p_o + p_j} \right) = \frac{B_o A}{2\eta L} \frac{(p_i^2 - (p_o + p_j)^2)}{(p_o + p_j)^2} M p \quad (2)$$

The error due to the backpressure at the jet can be calculated in terms of the ratio

$$\frac{F_j M p}{(p_o + p_j)} \bigg/ \frac{F_o M p}{p_o} = \frac{F_j p_o}{F_o (p_o + p_j)} = \left( \frac{p_i^2 - (p_o + p_j)^2}{p_i^2 - p_o^2} \right) \frac{p_o^2}{(p_o + p_j)^2} \quad (3)$$

Since  $p_o$  is fixed and  $p_j$  is almost constant during each run, it is more convenient to neglect terms in  $p_o/(p_o + p_j)$  and consider only the ratio

$$\frac{F'_o}{F_o} = \left( \frac{p_i^2 - (p_o + p_j)^2}{p_i^2 - p_o^2} \right) \quad (4)$$

which reduces to 1.0 for  $p_i \gg p_o > p_j$ . Values of eqn. 4 are given in Table I for  $p_o = 14.7$  p.s.i.g. Typically the experimentally determined backpressure amounted to 0.2 p.s.i.g.

As a check of the measured flow rates it is convenient to replace eqn. 1 by the form

$$F_o = \frac{B_o A p_o}{2\eta L} \left( \left( \frac{p_i}{p_o} \right)^2 - 1 \right) \quad (5)$$

Values of the term in brackets are given in Table I.

TABLE I

EFFECT OF BACKPRESSURE ON FLOW RATE RATIO  $F_o'/F_o$  (EQN. 4)

$p_i$ (p.s.i.g.)	$(p_i/p_o)^2 - 1$	Backpressure (p.s.i.g.)				
		0.1	0.2	0.3	0.4	0.5
5	0.7960	0.983	0.966	0.948	0.931	0.913
10	1.8233	0.993	0.985	0.977	0.970	0.962
15	3.0820	0.996	0.991	0.987	0.982	0.978
20	4.5722	0.997	0.994	0.991	0.988	0.985
25	6.2937	0.998	0.996	0.993	0.991	0.989
30	8.2466	0.998	0.997	0.995	0.993	0.992

*Current-voltage curves for the FID*

The form of the current-voltage curves for the FID, at a constant rate of sample addition, is now quite familiar. A steep rise in current is obtained at low voltages and a plateau at higher voltages (Fig. 5), the latter corresponding to collection of all the ions formed in the flame<sup>2</sup>. At still higher voltages the signal may increase again<sup>6,14</sup> and this point will be discussed briefly later. The curves for the jet positive and jet negative differ slightly, the difference being a function of the detector geometry and hydrogen flow rate<sup>15</sup>.

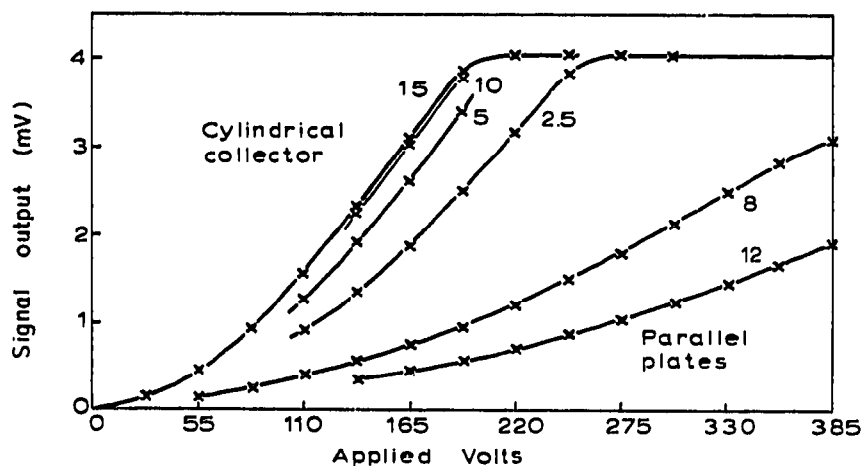


Fig. 5. Current *vs.* voltage curves for cylindrical and parallel plate electrode systems. Numbers on the upper curves represent the cylinder length in mm, on the two lower curves the distance between the plates in mm.

The voltage required to reach saturation is dependent on the saturation ion current, and it has recently been shown<sup>15</sup> that below saturation the current *vs.* voltage ( $i/V$ ) curves for the cylindrically symmetrical FID and a positive jet can be described by the relationship (given in MKS units)

$$V = \left( \frac{i}{2\pi k_1 \epsilon_0} \right)^{1/2} (a - b) \left( 1 + \frac{b}{a} \left( C \frac{i}{I} - 1 \right) \right)^{1/2} \quad (6)$$

where  $a$  is the collector radius,  $b$  is the outer radius of the ion formation and recombination region (approximately 1 mm for a 20 g jet),  $C$  is a constant (approximately

3.0),  $k_1$  is the mobility of the positive ions, and  $\epsilon_0$  is the permittivity of free space ( $8.854 \times 10^{-12}$  farad meter<sup>-1</sup>).

Below the saturation voltage the current is a function of the applied voltage, and only above the saturation voltage can a linear relationship between ion current and additive flow rate be expected. If the applied voltage is sufficiently low the term  $C (i/I)$  in eqn. 6 will be negligible, and the measured current will be independent of the saturation current and therefore independent of the concentration of organic additive.

In deriving eqn. 6 it is assumed that the measured ion current is small in comparison with the saturation current, but in practice it is found that there is good agreement with the experimental curves up to at least 70% of the saturation level. In fact, the use of the equation can also be extended to the saturation point for which  $i = I$ . It is then seen that the voltage required to reach saturation will be proportional to the square root of the saturation ion current, or of the mass flow rate of organic additive if the detector response is linear. Experimental results confirming this relationship are shown in Fig. 6. The lines drawn through the points correspond to a square law relationship. Both the coaxial cylinder and single flat plate collector electrode systems<sup>2,16</sup> are seen to obey the square law relationship but the greater ion collection efficiency of the cylindrical electrode is clearly shown. For both hydrocarbons and oxygenated organic compounds the results are independent of the compound itself, and are dependent only on the ion concentration and the geometry of the system<sup>15</sup>. It is also found that saturation is reached at a lower voltage if the jet is positive with respect to the collector electrode than if it is negative.

Eqn. 6 further predicts that the saturation voltage will be a function of the collector diameter, and this relationship has also been confirmed experimentally<sup>15</sup>. It might be thought that the length of the collector electrode would have a pronounced effect on the ion collection efficiency, but this is a secondary consideration as shown by the curves of Fig. 5. In fact, with short collectors precise vertical positioning is more important than length. Also shown in Fig. 5 are some results obtained with parallel plate collectors, of relatively large area and spaced 8 and 12 mm apart. It is

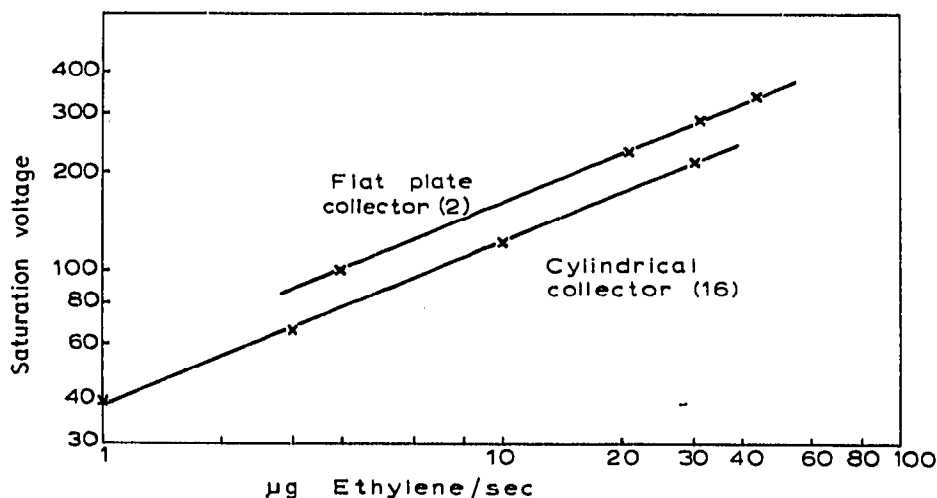


Fig. 6. Relationship between saturation current and mass flow rate of organic additive (log scales).



seen that the collection efficiency obtained with the cylindrical collector is far superior to the parallel plate system.

#### *The effect of the jet temperature*

The current *vs.* voltage curves shown in Fig. 5 apply under normal conditions when the jet is relatively cool. At high hydrogen and low nitrogen flow rates the heat released from the flame may cause the jet to become red hot. To avoid these conditions, which result in excessive noise and a very large background signal, relatively massive jets to provide good heat conduction from the jet tip are commonly used with pure hydrogen<sup>1, 14</sup>.

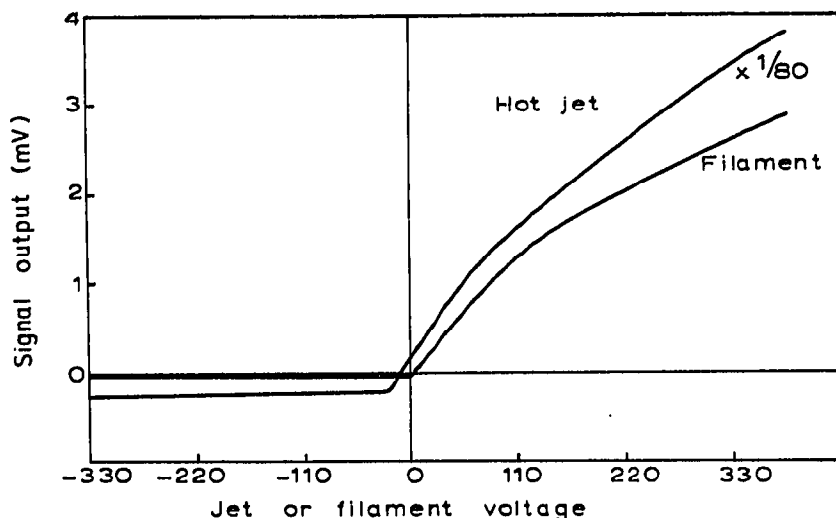


Fig. 7. Current *vs.* voltage curves for the hot jet (hydrogen flow rate 35 ml/min) and for a heated filament suspended in air.

Current *vs.* voltage curves obtained with hydrogen only and without further addition of organic material are shown in Fig. 7. Saturation is reached with the jet negative (corresponding to movement of the negative ions to the outer "collector" electrode) but this saturation current increases rapidly with increasing hydrogen flow rate. At low flow rates (below 40 ml/min) the signal was found to increase at approximately the fourth power of the hydrogen flow rate, but at about 75 ml/min a maximum was reached corresponding to a saturation current of  $10^{-9}$  A. Above 25 ml/min the jet glowed a bright red and even at the lowest flow rates a faint red glow was discernable. At higher flow rates the flame was a faint orange colour and completely surrounded the jet tip. This is in marked contrast to a hydrogen-nitrogen flame which cannot be seen without the addition of organic contaminants and is well separated from the jet. It is probable that the observed current can be directly related to the jet temperature, and a visible decrease in temperature occurs at flow rates above that corresponding to the current maximum. With the jet positive there is a steady, almost linear, increase in signal with increase in applied voltage (Fig. 7). These results are similar, but apparently not identical, to those obtained with a heated filament suspended in air, as shown in Fig. 7. Such behaviour has been ascribed to the emission of positive ions by the filament material<sup>17</sup> and extension of this argument to the heated jet of the FID is not unreasonable.

At high concentrations of organic additives a different phenomenon is observed. Thus it has been reported that at high ion currents and high applied fields electron multiplication occurs giving rise to a steep increase in ion current above the saturation level as the voltage is increased. With the present detector and a 13 mm I.D. collector electrode this effect has not been observed under normal operating conditions at voltages up to 380 V and ion currents up to  $10^{-6}$  A, the latter being several orders of magnitude higher than those at which very pronounced effects have been reported<sup>6, 14</sup>. However, during some of the early linearity checks it was found possible to obtain this type of response at high hydrogen and low nitrogen flow rates which result in the jet becoming red hot.

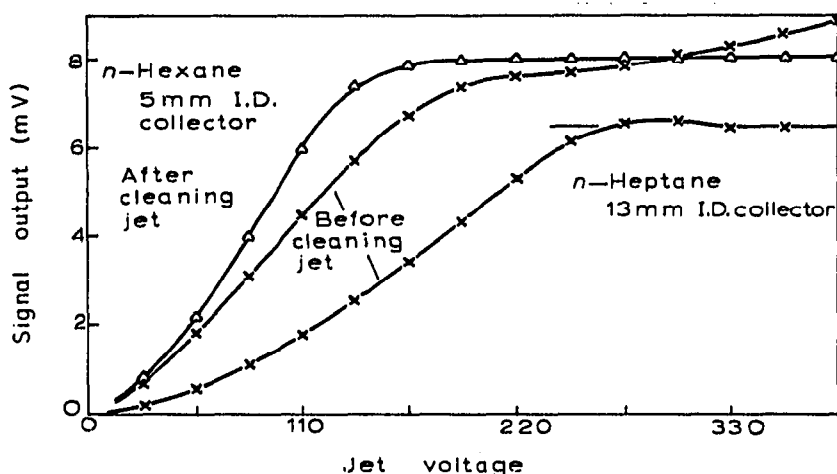


Fig. 8. Current *vs.* voltage curves at high additive concentrations, showing effects of jet contamination.

Subsequently, anomalous results were observed in the current *vs.* voltage curves for *n*-heptane at high ion currents, the current reaching an initial peak above the true plateau level (Fig. 8). This behaviour was accompanied by a sharp rise in the observed current on reducing the voltage, the change being a "metastable" one in that the current again fell to its original level after a short time interval. The latter was critically dependent on both the hydrogen and additive flow rates. It was also found that under these conditions a rapid increase in ion current with applied voltage was obtained with *n*-hexane and a 5 mm I.D. collector electrode (Fig. 8). This rise was independent of the collector material. Further consideration of possible causes of this behaviour led to cleaning of the jet with fine energy paper. As a result both the anomalous metastable response and any further increase above the plateau level disappeared.

Since it was observed that the tip of the jet had been covered with a carbon layer it seemed possible that this behaviour might be related to carbon deposition on the jet. However, depositing carbon on the cleaned jet from a smokey flame did not affect its performance. Oxidation of the metal is also a logical cause in the case of a stainless-steel jet, but this is unlikely to provide an explanation for the similarity in behaviour observed with both stainless-steel<sup>6</sup> and platinum<sup>14</sup> jets. Nevertheless, it seems evident that a surface phenomenon must be involved, even if only as a source of electrons or ions for subsequent multiplication effects. The fact that the increase

is not observed when the jet is negative suggests that it cannot be due to electron emission, but this evidence by itself cannot be regarded as conclusive.

### Linearity of response

The main purpose of the present study was to check the linearity of response of the FID at relatively high concentrations of organic additives. Initially, the hydrogen flow rate was adjusted to give the maximum signal output for a given additive flow rate<sup>2</sup>. This was done to ensure that small changes in either the hydrogen or total nitrogen flow would have a negligible effect on the final results. Subsequently, the effect of substantial changes in the hydrogen flow rate was further investigated and these results are also reported below.

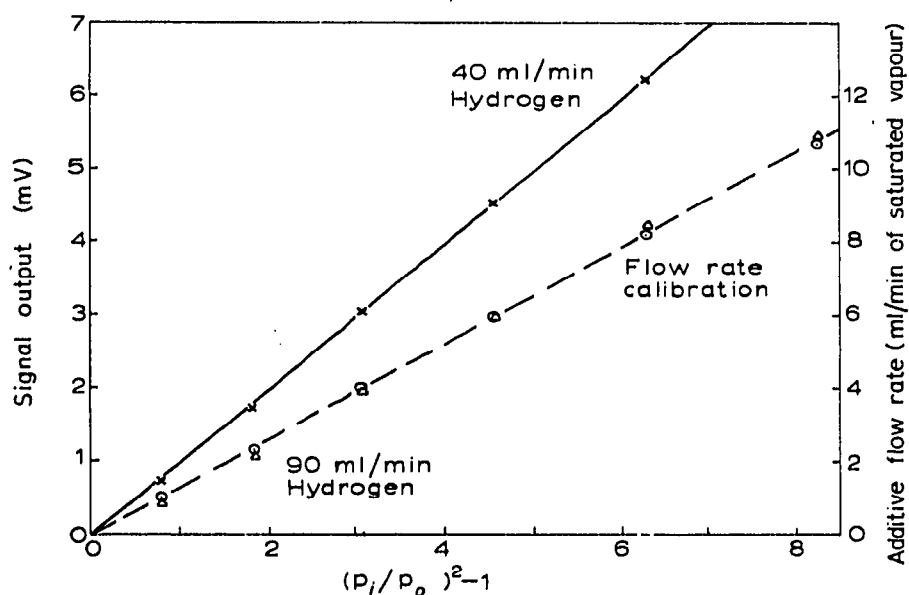


Fig. 9. Linearity of response for *n*-heptane and flow calibration check.

In Fig. 9 the upper line shows the results obtained for *n*-heptane at flow rates through the saturator from 1 to 10 ml/min. The signal output is plotted against the flow term  $[(p_i/p_o)^2 - 1]$ , eqn. 5, and the flow rate through the saturator (broken line) is also plotted on the same scale. The slight deviations of the experimental points from a straight line are consistent in both sets of results, indicating that this is due to small errors in the pressure gauge calibration. After correction for this and for the backpressure at the jet, it is found that the detector is linear over the range shown to within the accuracy of the experimental results, estimated to be better than  $\pm 1.5\%$  overall.

The experimental points shown by the triangles in Fig. 9 are of particular interest since these correspond to a non-linear form of response similar to that reported elsewhere for a detector with a relatively massive jet, designed for use with capillary columns and hydrogen carrier gas<sup>14</sup>. The present results were obtained at a high hydrogen flow rate, although insufficient to cause visible heating of the jet. It is therefore concluded that this non-linearity is associated with a high hydrogen concentration at the jet and is not caused simply by over-heating of the jet. Nevertheless the con-

sequences are self-evident; if hydrogen is used as a carrier gas it is necessary to add nitrogen or a similar diluent to the gas stream entering the detector to preserve linearity at higher concentrations.

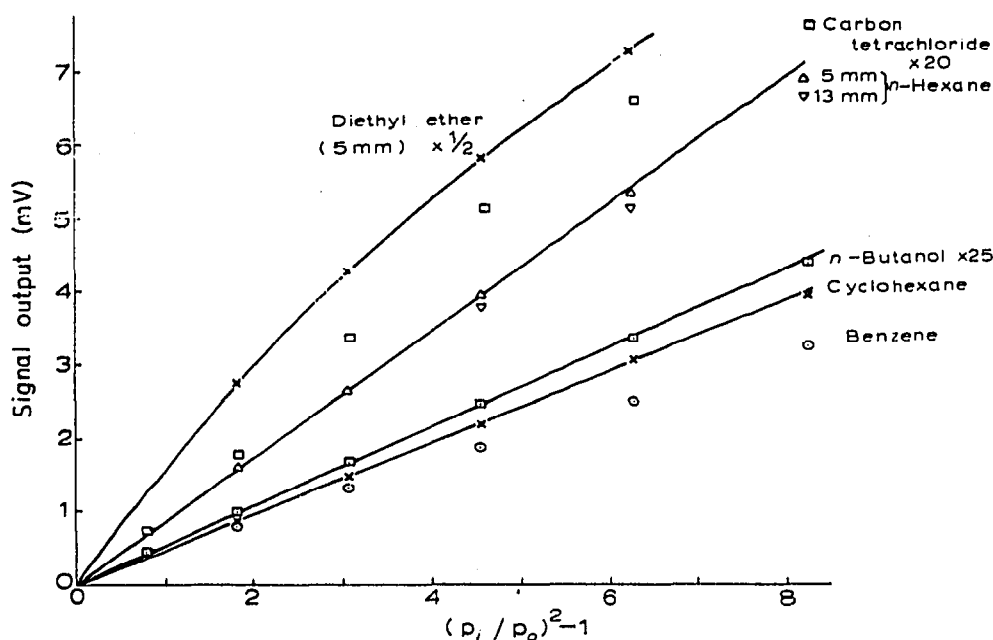


Fig. 10. Linearity of response for various additives.

Further linearity results under near optimum conditions for a number of other compounds are shown in Fig. 10. Benzene and carbon tetrachloride are of interest in that non-linearity becomes evident at much lower concentration levels with these compounds than with aliphatic hydrocarbons<sup>18</sup>. This is evident in comparing the results for benzene and cyclohexane which correspond to a similar signal output. For further comparison and reference purposes Table II gives the approximate mass flow rates corresponding to the second (10 p.s.i.g.), fourth (20 p.s.i.g.) and sixth point (30 p.s.i.g.) on each of the plots in Figs. 9–11. Carbon tetrachloride shows very pronounced non-linearity at ion currents above about  $6 \times 10^{-9}$  A but some improvement may be obtained by increasing the hydrogen flow rate. Thus, it has been found that the linearity of ethyl bromide (not shown in the figures) is improved at higher hydrogen flows, and this may well be a general effect for all halogenated compounds. This point is discussed further below and in the next section.

The results for *n*-butanol are taken from earlier work<sup>15</sup> carried out with the equipment described here, and cover a concentration range approximately twenty times lower than that for cyclohexane. At the other extreme are the results for *n*-hexane and diethyl ether, also from an earlier investigation. The departure from linearity of the *n*-hexane results at medium concentrations, with a 13 mm I.D. collector electrode, was due to failure to reach the saturation current level with an applied voltage of 380 V. This was remedied by using a 5 mm I.D. collector, but a slight residual deviation remains at the higher concentrations. The results for diethyl ether have been corrected for saturator inefficiency (Fig. 4) but they can only be regarded as approximate. Nevertheless the departure from linearity at these con-

TABLE II

REFERENCE DATA FOR FIGS. 9-11

Compound	Mol. wt.	V.p. <sup>a</sup> (mm)	Fig.	Flow rate ( $\mu\text{g}/\text{sec}$ ) corresponding to		
				10 p.s.i.g.	20 p.s.i.g.	30 p.s.i.g.
Diethyl ether	74	440	10	(73)	(188)	(341)
<i>n</i> -Hexane	86	121	10	23	60	(109)
Cyclohexane	84	78	10	15	38	(69)
Benzene	78	74	10	(13)	(33)	(60)
<i>n</i> -Heptane	100	35	9	7.9	20	37
Toluene	92	22	11	4.6	11.7	21
<i>n</i> -Butanol	74	5.0	10	0.8	2.1	3.9
Carbon tetrachloride	154	88	10	(31)	(78)	(142)

<sup>a</sup> At 20°: estimated from data given in *Handbook of Chemistry and Physics*, The Chemical Rubber Co., Cleveland, 1969, p.D-148. Figs. in brackets correspond to a non-linear response.

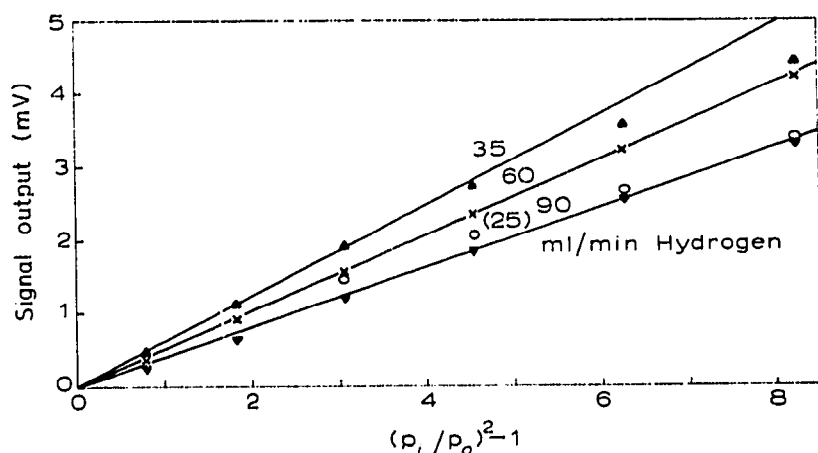


Fig. 11. Linearity of response for toluene at different hydrogen flow rates.

centration levels is quite evident. Once again a 5 mm collector electrode was used and inefficient ion collection did not contribute to these results.

As with benzene (Fig. 10) the linearity of response for toluene is relatively poor at hydrogen flow rates below or at that corresponding to the maximum signal output. This is shown in Fig. 11 by the results corresponding to hydrogen flow rates of 25 and 35 ml/min. However, increasing the hydrogen flow rate still further to 60 ml/min resulted in a considerable improvement in linearity as is shown in the figure. At still higher flow rates (90 ml/min) an alternating effect is observed similar to that obtained with *n*-heptane at high hydrogen flow rates (Fig. 9).

#### The effect of the hydrogen flow rate

The departure from linearity with a large increase in hydrogen flow rate has already been mentioned in the previous section for the cases of *n*-heptane and toluene. This behaviour has been further investigated by examination of the signal *versus* hydrogen flow rate curves at several concentration levels. This was done by repeatedly injecting fixed volumes of gas sample into a chromatograph with a Carle gas sampling valve and varying the hydrogen flow to the detector. Up till the present time it has

been assumed that the optimum hydrogen-nitrogen ratio is independent of the compound type, and the only reported work in this area supports this view<sup>3</sup>. However this is not always so, although it is generally a sufficiently close approximation at low concentrations (Fig. 12). As the concentration of organic additive increases there is a shift in the maximum to higher hydrogen flow rates, and this is shown for *isopentane* in Fig. 13. Also included in this figure are some results for carbon tetrachloride, which show a very pronounced departure from the normal behaviour. At higher concentrations a peak maximum is observed.

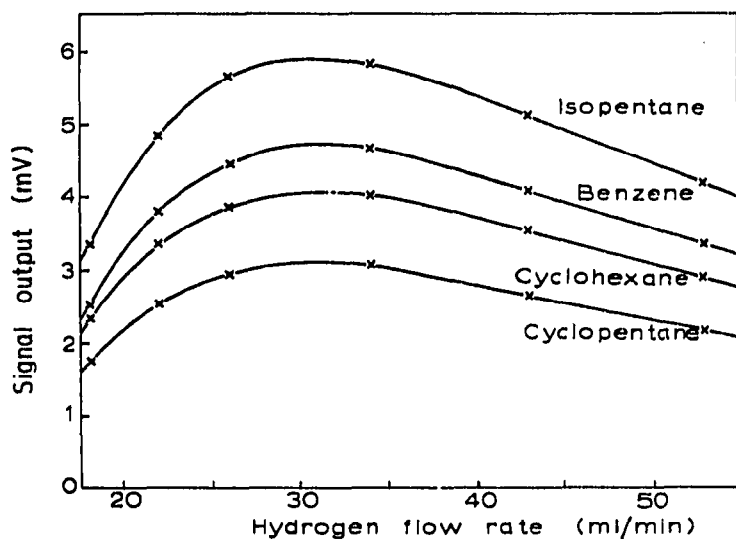


Fig. 12. Effect of hydrogen flow rate on response, for various compounds at low concentrations (by chromatographic analysis).

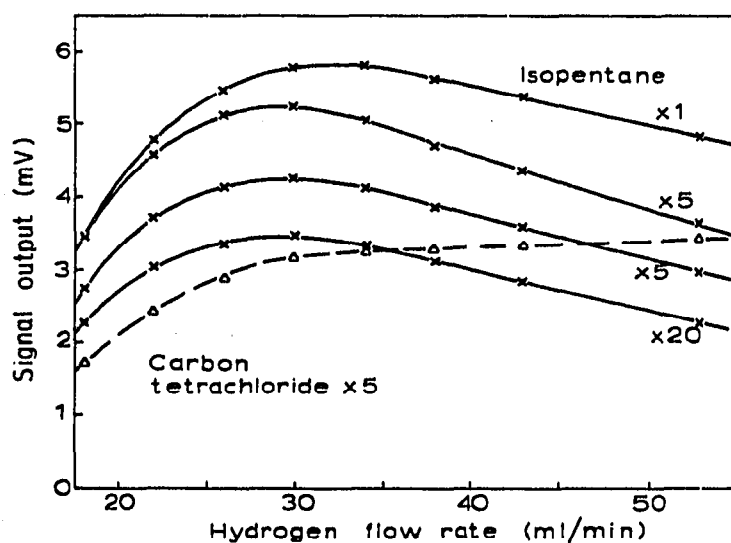


Fig. 13. Effect of concentration and hydrogen flow rate on the response of isopentane (by chromatographic analysis).

Fig. 14 shows the shift in the peak maximum with increased additive concentration for a number of different compounds, each being measured at two concen-

tration levels. The straight connecting line between these two levels does not necessarily imply that a linear shift occurs with increased concentration, but is used merely to simplify the diagram. This shift can of course have a pronounced effect on linearity of response, and may also help to explain the strange changes in relative responses which have been reported for different detectors and different hydrogen flow rates<sup>14, 19</sup>. However, it is evident from Fig. 13 (and from Fig. 12 at low hydrogen flow rates) that even at low concentrations the relative responses may be dependent on the hydrogen flow rate.

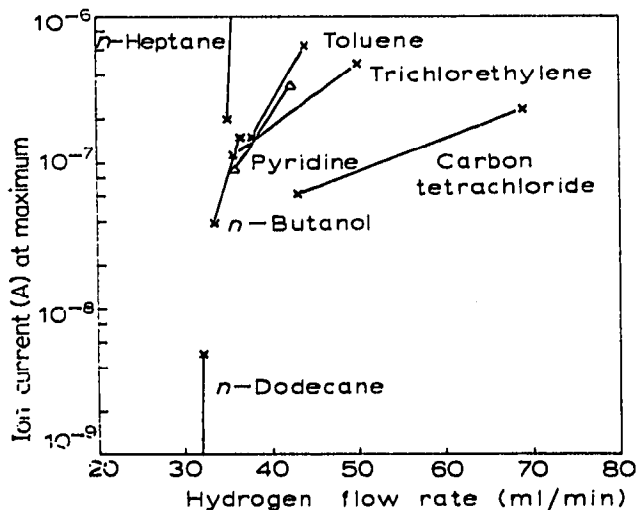


Fig. 14. Effect of compound type and concentration on the hydrogen flow rate required for maximum signal output (nitrogen flow rate 35 ml/min).

It is tempting to try to relate the above shift to the molecular structure of the compound, but insufficient data have been obtained so far for a serious attempt to be made. Nevertheless it is evident that the displacement is most pronounced with aromatic and non-hydrocarbon compounds, and the largest shift so far observed is for carbon tetrachloride. Data obtained at three different total nitrogen flow rates (35, 60 and 90 ml/min) suggest that the shift, measured in ml/min of hydrogen, is almost independent of the nitrogen flow rate over this range. The observed shifts for the two chlorinated compounds are much greater than could be explained on the simple basis of the hydrogen required to convert all the chlorine in the molecule to hydrogen chloride, or indeed for total conversion of the compound to methane and hydrogen chloride. On the other hand, a relationship based on burning velocity considerations<sup>6</sup> also appears to be untenable in view of the observation that carbon tetrachloride has only a small effect on the burning velocity of a hydrogen-air flame, much less than that of saturated hydrocarbons or aromatics<sup>20</sup>.

#### ACKNOWLEDGEMENT

This work was made possible by the award of a Research Fellowship by the Shell Group of Companies in Australia.

## REFERENCES

- 1 D. H. DESTY, C. J. GEACH AND A. GOLDUP, *Gas Chromatography*, Butterworths, London, 1960, p.46.
- 2 I. G. MCWILLIAM, *J. Chromatog.*, 6 (1961) 110.
- 3 R. J. MAGGS, *Column*, 1 (2) (1966) 2.
- 4 J. M. GILL AND C. H. HARTMANN, *J. Gas Chromatog.*, 5 (1967) 605.
- 5 H. OSTER AND F. OPPERMAN, *Chromatographia*, 2 (1969) 251.
- 6 J. C. STERNBERG, W. S. GALLAWAY AND D. T. L. JONES, *Gas Chromatography*, Academic Press, New York, 1962, p. 231.
- 7 R. W. ROSKE AND D. H. FULLER, *ISA J.*, 10 (3) (1963) 73.
- 8 J. KRUGERS, *Philips Res. Rep., Suppl. 1*, 20 (1965) 70.
- 9 B. A. SCHAEFER, personal communication.
- 10 P. D. SCHNELLE, *ISA J.*, 4 (4) (1957) 128.
- 11 L. ANGELY, E. LEVART, G. GUIOCHON AND G. PESLERBE, *Anal. Chem.*, 41 (1969) 1446.
- 12 G. S. TURNER AND W. M. CRUM, in L. FOWLER, R. D. EANES AND T. J. KEHOE (Editors), *Analysis Instrumentation, 1963*, Instrument Society of America, Pittsburgh, 1963, p. 77.
- 13 H. PURNELL, *Gas Chromatography*, Wiley, New York, 1962.
- 14 H. BRUDERREK, W. SCHNEIDER AND I. HALASZ, *Anal. Chem.*, 36 (1964) 461.
- 15 H. C. BOLTON AND I. G. MCWILLIAM, *Proc. Roy. Soc.*, in press.
- 16 R. A. DEWAR, *J. Chromatog.*, 6 (1961) 312.
- 17 B. E. HUDSON, W. H. KING AND W. W. BRANDT, *Gas Chromatography*, Academic Press, New York, 1962, p. 207.
- 18 Hewlett-Packard, *Series 5750B Research Gas Chromatograph Operating and Service Manual*, 1968, p. 2-6-11.
- 19 O. HAINOVA, P. BOČEK AND J. JANÁK, *J. Gas Chromatog.*, 5 (1967) 401.
- 20 D. R. MILLER, R. L. EVERS AND G. B. SKINNER, *Combust. and Flame*, 7 (1963) 137.

*J. Chromatog.*, 51 (1970) 391-406